STRUCTURAL DESIGN OF SERPENTINE GAS CHANNEL IN FUEL CELL

Nawras H. Mostafa **Qusay R. Al-Hagag**

التصميم البنيوي للقناة الغازية الملتفة في خلية الوقود

الخلاصة

تعتبر صفيحة تحرير كل من الوقود و الغازات المؤكسدة أو ما يسمى بصفيحة خلية الوقود، الجزء الرئيسي لخلية الوقود ذات غشاء التبادل ألبروتوني. ولأجل تطوير أداء صفيحة خلية الوقود مع تقليل كلفتها، تم استخدام طريقة العناصر المحددة للتحليل البنيوي و الحاسوب عالي النمذجة كأداة نافعة لتحسين صفائح خلايا الوقود في الوقت الحالي.

خلال عمل خلية الوقود، يتم رفع درجة حرارة الصفائح إلى 80 درجة مئوية و بشكل متكرر مع وجود أحمال بنيوية. هذه الحرارة تؤدي بالنتيجة إلى تكوين اجهادات حرارية أعلى من اجهادات التحميل البنيوي. لهذا فأن الاجهادات الحرارية تلعب دوراً أساسيا في التصميم البنيوي لتلك الصفائح.

تم تحليل صفيحة من النوع الملتف باستخدام طريقة العناصر المحددة في حالة المرونة الخطية و اللاخطية. تم تطبيق كمالية التصميم و ذلك لتقليل أعظم إجهاد ضمن صفيحة خاضعة لتقييد في الأبعاد الهندسية وفي خواص المادة كمتغيرات تصميمية. أظهرت الدراسة مميزات الصفائح المطبوعة و طريقة تصميم صفيحة خلية الوقود.

ABSTRACT

Fuel and oxidant gas delivery plate, or fuel cell plate, is a key component of a Proton Exchange Membrane (PEM) fuel cell. To develop low-cost and high performance fuel cell plates, advanced computer modeling and finite element structure analysis are used as useful tools for the optimization of the plates at the early design stage.

In a fuel cell application, these fuel cell plates are routinely heated up to $80^{o}C$ with structure pressure loads. The temperature induced thermal stresses is found to be much higher that the structure loading stress. Thus, the thermal stresses plays a key role in the structure design and optimization of the plates.

To carry out the analysis, a model of the serpentine plate is analyzed using finite element analysis model for both linear and nonlinear elasticity analysis. Design optimization is applied to minimize the maximum stress within the plate, subject to constraint with both geometry and material parameters as design variables. The study reveals the characteristics of the printed plates, and provides guidelines for the structure and material design of the fuel cell plate.

Keywords / gas channel fuel cell, stresses analysis, design optimization, linear and nonlinear analyses, FEA model

1-INTRODUCTION

Fuel cell, as an electrochemical device that applies hydrogen fuel and oxidant air to produce electricity, is considered as a zero-emission option to reduce air pollution and greenhouse effect. Polymer Exchange Membrane (PEM) fuel cell is a promising alternative to the automotive internal combustion engine as a clean power plant due to its light weight, low operation temperature, and high efficiency. However, one of the major obstacles to the commercialization of PEM fuel cell is its high cost. Fuel cell stack, which is made of many single fuel cells, is the core of the automotive power plant. The single PEM fuel cell compromises a membrane electrode assembly (MEA), and two gas delivery plates, which provide the hydrogen fuel and oxidant air to the cells as shown in **Fig.1**. At present, the gas delivery plates are made mostly through computer numerical control (CNC) machining, although molding, pressing and many other are being developed and tested [Pastula, 1997]. The machining method requires slicing, cutting, grinding and polishing, and leads to unreasonably high manufacturing costs. This high cost including manufacturing process and materials accounts about 25% of the whole PEM fuel cell system.

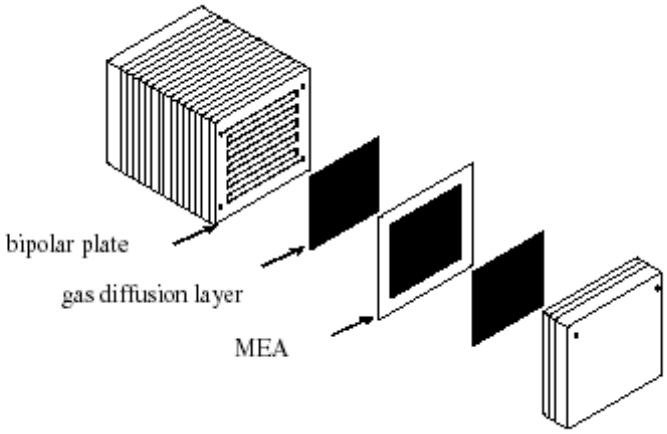

Fig.1: Polymer electrolyte membrane fuel cell stack with gas channels [mennola, 2000].

A variety of polymer and graphite composites have been reported, some of which promise low costs and injection mold ability. Busick & Wilson [1998] describe a composite material with a material cost of $3/kg. A cost of $10/kg for the final plate is believed to be attainable. At a power density of 1 kW/kg, the cost due to bipolar plates would thus be $10/kW, assumed that the mass of the stack consists mostly of bipolar plates. This still exceeds the target of $4-6/kW. In addition, it is not clear whether the power density of 1 kW/kg can be achieved with composite plates. Composite materials typically have a lower electric conductivity than solid graphite, resulting in higher ohmic losses. In addition, their mechanical strength may be a problem. Another composite material is reported by Onischak [1999]**.** The material reported offers performance comparable to solid graphite and due to its inherent flexibility should actually allow thinner plates than those made of solid graphite. The projected cost of bipolar plates in high-volume production is $10/kW. Steel plates are mechanically durable and thus bipolar plates made of steel could be made very thin. Steel is also a very cheap material. The alloy most commonly used in fuel cells is SS316. Problems include high contact resistances due to an oxide layer on the surface. In addition, corrosion may be a problem in long-term performance. Because of this, it is generally regarded that a low resistance surface coating is needed [Reid *et al.,* 1998]. The necessity of coating has been questioned by Davies *et al.* [2000]**,** who claim that the cost can outweigh the performance gain. They also state

that endurance testing of uncoated steel in excess of 3000 hours has been successfully conducted. Therefore the cost issue dominates the fuel cell plate development. The cost of a new product consists of the development cost and manufacturing cost. Conventional product development is carried out through a trial and error process requiring many design and prototyping iterations [Menon 1998]. The lengthy design lead-time leads to high cost at the early stage of product development. The manufacturing cost of a product depends on its design, and the material used. All of these two aspects have to be addressed in order to lower the cost of a fuel cell plate.

This study applies the finite element analysis (FEA), on the fuel cell plate structure design that covers both plate geometry and plate material. Conventionally, most computational structure design deals with only geometry, which focuses on the shape of the design for mature materials with known performance. In this study, the material and its properties for the fuel cell plate is also to be determined. The purpose of fuel cell plate structure design is to obtain an improved fuel cell gas delivery plate with certain materials based on the screen-printing manufacturing method. The optimal design will provide the ideal geometry of structure and broader material performance for the materials development. The design optimization of plate geometry is carried out using key geometry parameters as design variables. The material design uses both geometry parameters and the key material parameter, the Young's modulus, as design variables. Both of the geometry design and material design are conducted by minimizing the maximum stress within the plate, subject to the maximum strain allowed. The FEA structure simulation includes linear elasticity analysis, nonlinear elasticity analysis, prestress analysis. These analyses are used as measurements of design objectives and constraints in the optimization.

2. COMPUTATIONAL MODELING

2.1. Solid Modeling

The model of the fuel cell gas delivery plate is illustrated in **Fig.2**. The linked parallel channels are connected to an air inlet and an air outlet at each end. The parametric solid model of the plate is constructed as a rectangular shaped building layer structure, as shown in **Fig.3**. The key design parameters of this solid model include: thickness of the printed layer, *H*, channel wall thickness *W*, and channel length, *D*. These parameters are used later as design variables in the optimization.

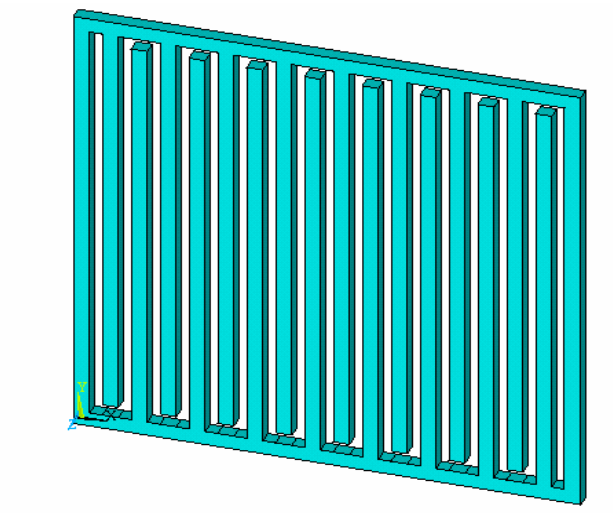

Fig.2. Simplified fuel cell flow channels

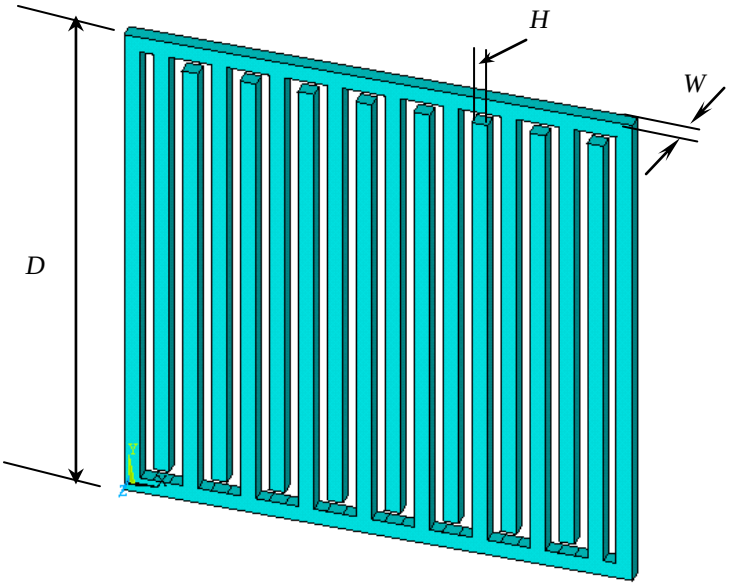

Fig. 3. Parametric solid model of fuel cell flow field layer structure

2.2. FEA Structure Model

The finite element analysis is used to calculate the stress and strain in the printed channel wall with the assumption of a good adhesion between the building layer and the substrate. The model consists of a solid substrate (graphite or coated metal) with a "printed" flow-field channel wall layer (polymer-based composites). A uniform steady temperature distribution is assumed at any temperature step. The zero stress state or the initial condition for the calculation is at room temperature. The temperature of the entire plate is raised up to 80^{o}C to simulate the working condition of the PEM fuel cell [Al-Hagag, 2005].

Thermal stress is induced by the heating process due to the mismatch of the substrate and the printed channels with different thermal expansion coefficients. Since the polymer and polymer composites are quite thermal sensitive within this temperature range, nonlinear finite element analysis might be needed. The calculation is carried out by first using a linear FEA model, then to determine whether geometry nonlinearity and/or materials non-linearity needs to be applied and to calculate again if a nonlinear model is needed. For the fuel cell application, the plate has to undertake repeated temperature loads and structure loads. Both linear and nonlinear analyses are thus based on the elasticity assumption.

One significant issue in the structure model is that the composite material used in this study itself is also being developed. Due to the rigorous chemical stability and conductivity requirements of the plate, graphite and carbon are major ingredient materials for the substrate and the flow channels with different binders, leading to different thermal expansion rates and thermal stress. The structure is subject to the similar issues faced by surface mounting and thin film deposition in the electronic industries [Pirondi,1998]. The stress or strain will induce failures that directly affect the reliability of the printed plates [Shi1,995] and its ability to delivery fuel and oxidant gas in fuel cell operation. The unknown composite material during the design determines that the structure design has to follow a special procedure used in this study.

3. DESIGN OPTIMIZATION

In this work, the design optimization is carried out for both plate geometry and material. Two different design objectives and two different sets of design variables are used in tandem. The most challenging issues facing the fuel cell plate material development are good conductivity, excellent electro-chemistry stability, sound structure integrity and low cost. Three key material properties, maximum stress, maximum strain, and stiffness, are directly related to the structure design requirement. For composite material development, minimum yield stress, minimum failure strain, and minimum Young's modulus will support a broader selection of composite material composition.

The maximum von Mises stress relates to the lifetime of the structure. By selecting the minimum maximum von Mises stress, σ_{vm}, as the objective function, the optimal design will provide lowest material strength requirement, which the new developing composite material should be reached. Another material performance, maximum 1st principal strain, ε^1, is defined as a constraint for the optimization to satisfy material deformation restriction. The selections of design variables are made for two different considerations, plate geometry and plate materials, as discussed in the following subsections.

3.1. Geometry Design

In the plate geometry design optimization, traditional geometry parameters are used as design variables. The material parameters are assumed to be constants with their values determined from similar materials. The optimization considers the worst-case condition, minimizes the maximum von Mises stress, σ_{vm}, of the structure, subject to the constraint of the maximum strain level [ε^1], the maximum allowed 1st principal strain ε^1. These stress and strain are evaluated using the ANSYS finite element analysis model. The optimization is carried out using two key variables for the plate geometry: the wall thickness, *W*, and the thickness of the printed layer, *H*, as shown in **Fig.3**. The optimization is defined as:

$$\min_{W,\,H} \sigma_{vm} . \tag{1}$$

$$\textit{subject to: } \varepsilon^1 \leq [\varepsilon] \tag{2}$$

where the design variables, $\boldsymbol{X=[W, H]^T}$.

3.2. Materials Design

In the plate material design optimization, both geometry parameters and the material performance parameter of the plate are used as design variables. By adding the material stiffness as design variable, the optimal design will find the ideal value of the stiffness (or the Young's Modulus) of the composite material. The optimization shares the same objective and constraint functions of the plate geometry optimization.

The optimization is carried out using three key variables for the plate geometry and material: the wall thickness, *W*, and the height of the printed layer, *H*, and the material stiffness (or Young's Modulus), *E*. The optimization is defined as:

$$\min_{W,H,E} \sigma_{vm} . \quad (3)$$

$$\textit{subject to}: \varepsilon^{1} \leq [\varepsilon]$$

where the design variables, $X=[W, H, E]^T$.

4. RESULTS AND DISCUSSION

4.1. FEA Structure Analysis

The geometry model in **Fig.2**, is transferred to ANSYS to form the finite element analysis model. The design parameters of the deposited layer are listed in **Tables 1** and **2** below.

Table 1: Dimensions of the plate

Geometrical Parameters		
D (m)	*W* (m)	*H* (m)
0.055626	0.001651	0.001778

Table 2: Material properties of epoxy- based composites

Material Parameters			
mass density (Kg/m^3)	Young's modulus (GPa)	Poisson's ratio	coefficient of thermal expansion (m/m K)
1299.52	3	0.37	$6*10^{-5}$

Quadratic 10 node tetrahedral elements called SOLID92 are used for the model as shown in **Fig.4**. This element is defined by ten nodes having three degrees of freedom at each node: translations in the nodal x, y, and z directions. The element also has plasticity, creep, swelling, stress stiffening, large deflection, and large strain capabilities. Based on the geometry above, the total elements of 16362 are generated with high density at the end and corner areas as shown in **Fig.5**.

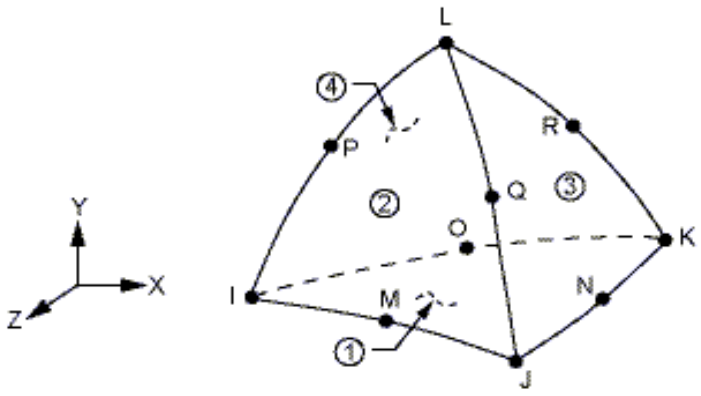

Fig. 4: SOLID92 Element (ANSYS Element Reference)

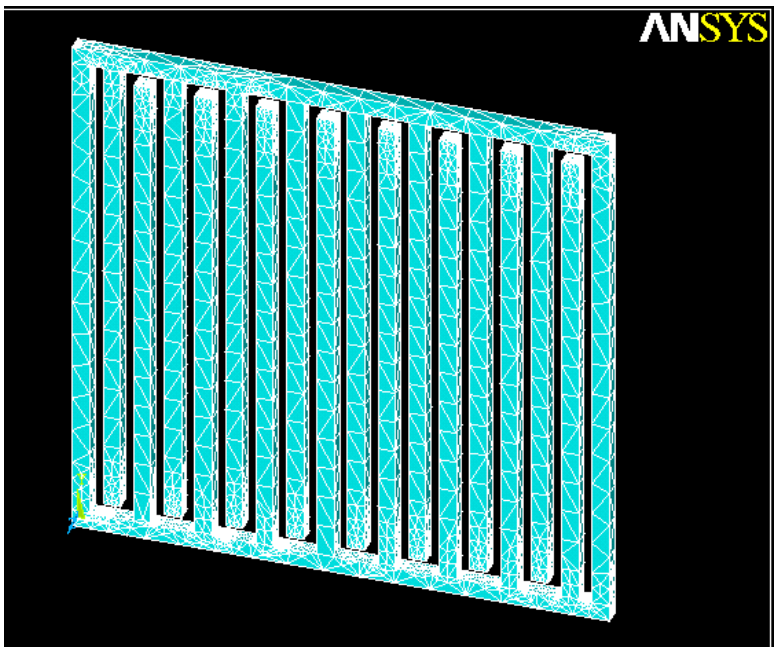

Fig. 5: Mesh generation of the model

The element input data includes the degree of freedom, material properties, surface loads such as pressures at each face for the element, and body loads such as temperatures at each node. Pressures may be input as surface loads on the element faces as shown by the circled numbers on Fig.4. Positive pressures act into the element. Temperatures may be input as element body loads at the nodes.

The analysis is first conducted using linear material elasticity analysis. The simulated plate is subject to inner channel pressure load, top uniform pressure, and temperature field. The result using different data sets of the analysis is shown in **Table 3**. Set (1) of this linear analysis is carried out with pure structure loads, including fixed bottom boundary condition, 204 *KPa* inner channel gas pressure, and 544 *KPa* uniform stack compressing top pressure, without a temperature field. Set (2) of the linear analysis covers only temperature load: fixed bottom boundary condition, and a 80^{o}C temperature field with 20^{o}C room temperature as reference, without any structure loads. Set (3) includes both structure and temperature loads: fixed bottom boundary condition, 204 *KPa* inner channel pressure, 544 *KPa* uniform top pressure, and a 80^{o}C temperature field.

Table 3: Linear and nonlinear structure analysis

Simulation Set	Max von Mises Stress (nodal)	Max. Displacement	Max. 1st Principal Strain(element)	Comment
(1) Structure loads only	1.28 *MPa*	0.481 μm	221 $\mu\varepsilon$	Safe
(2) Temperature load only	40.5 *MPa*	13.7 μm	8883 $\mu\varepsilon$	Unsafe
(3) Structure and temperature loads	41.4 *MPa*	13.9 μm	8931 $\mu\varepsilon$	Unsafe
(4) Temperature prestress	40.9 *MPa*	13.8 μm	8898 $\mu\varepsilon$	Unsafe
(5) Nonlinear	17.74 *MPa*	13.84 μm	7420$\mu\varepsilon$	Safe

According to the results on sets (1) and (2) from **Table 1**, the temperature induced thermal stress is much higher than that of the structure loads. In test (2), the epoxy-based composite material is working at a high stress level close to the material strength of 45-55 *MPa*. This may cause creep at the elevated temperature range. In addition, the temperature field effect generates relatively high maximum displacement and strain level. Test sets (1)~(3) indicate that the temperature field plays a key role on the maximum stress and strain occurred on the structure.

In a fuel cell, there is not a fixed order on the sequence of structure or temperature loads. In general, a higher stress loading has much more influence on the subsequent loading, compared to the lower stress loading. Thus, for this fuel cell plate application, the temperature field is first applied to generate the temperature pre stress, followed by the structure loads.

The temperature prestress simulation, set (4) is carried out through two load steps. The first temperature loading step is applied gradually from room temperature to 80^{o}C. Then the second structure-loading step is performed by gradually increasing the inner channel pressure and uniform top pressure from zero to 204 *KPa* and 544 *KPa*, respectively. Both load steps use 10 substeps to simulate the gradually increasing loading.

According to the results from set (3), the maximum strain level is 8898 $\mu\varepsilon$, less than 2%. The maximum displacement is 13.9 μm, which is only 0.84% of the shortest dimension, wall thickness *W*. Thus, no geometry nonlinearity needs to be considered in the model. However, the fix bottom condition provides a strong constraint. Therefore the stress stiffness effect associated with geometrical nonlinearity is considered at temperature prestress simulation in the simulation set (4) for more accurate analysis. The results show that the temperature prestress effect has 1.2% and 0.37% decrease on the maximum stress and strain, respectively, compared to the results from simulation set (3). Based upon these analyses, the high stress predicted by the model, or introduced by the selected plate structure and/or material, is undesirable.

One of significant issues for epoxy-based composite materials at 80^{o}C is the nonlinear stress-strain relation. The elasticity analysis of the nonlinear material considers nonlinear stress-strain relation instead of a single Young's modulus. The stress-strain relation, as a material performance characteristics input, is constructed using multiple linear segments, with the initial slope equal to the Young's modulus, and the rest segments following by a series of lines with decreasing slopes. For generality, the ratio of the original and following slopes of these line segments are 100%, 98%, 94%, 90%, 85%, 80%, etc. of the Young's modulus of 3*GPa*. The nonlinear materials elasticity simulation, set (5), follows the same boundary and loading conditions as the set (3) previously discussed.

The nonlinear materials elasticity analysis, set (5) of **Table 3**, produces a maximum von Mises stress17.74 *MPa*, a 1^{st} principal total strain 7420 $\mu\varepsilon$, and a maximum displacement 13.84 μm. These are within the working range for epoxy materials. The simulation also indicates that both maximum stress and maximum strain occurs at the fix corner and channel/wall ends, for all loading conditions. The results from simulation sets (1), (2) and (3) are shown in **Figs. 6**, **7**, and **8** respectively. In summery, the finite element analysis indicates that high stress level is induced by the temperature load. Material nonlinearity needs to be considered in the structure design. In addition, the corner effect of maximum stress and strain is important for the geometry design.

4.2. Optimal Geometry and Material Design

The structure optimizations of the plate include both geometry and material considerations. One of the built-in optimization functions of ANSYS, advanced zero order method or sub-problem method, is used for the plate structure optimization. The routine applies a search approach, in which a few sets of objective and constraint functions are approximated by several fitted surfaces. The optimization routine searches through the fitted surface, instead of the original function surfaces, to

improve search efficiency. The fitting controls use quadratic functions for the objective and constraint functions. This method of optimization can be described as an advanced, zero-order method in that it requires only the values of the dependent variables (objective function and state variables) and not their derivatives. The dependent variables are first replaced with approximations by means of least squares fitting, and the constrained minimization problem described is converted to an unconstrained problem using penalty functions. Minimization is then performed every iteration on the approximated, penalized function (called the sub problem) until convergence is achieved or termination is indicated. For this method each iteration is equivalent to one complete analysis loop. For more details about this method of optimization, see ANSYS documentation.

Design optimization is applied to both linear and nonlinear material analysis, based on the Simulation Sets (3) and (5) of **Table 3**, discussed previously. Based on the geometry design consideration of linear analysis set (3), the geometry parameters wall thickness, *W*, and layer thickness, *H*, in the structure model (**Fig. 3**) are chosen as design variables of the Design Set (1), which *W* ranging from 0.5 *mm* to1.8 *mm*; *H* ranging from 1 *mm* to 2 *mm*. The chosen starting point is at $W = 0.001651\ m$, and $H = 0.001778\ m$. The 1st principal strain is used as the design constraint with an upper limit at 12000 μm. The objective function, von Mises stress, is minimized.

In this optimization, all other items, i.e. Young's modulus $E = 3\ GPa$, are fixed same as the previous linear analysis simulation set (3). The search often ends prematurely at local optima. Many restarts are tested at different start points, including the identified true global minimum at $W = 0.00153\ m$ and $H = 0.00158\ m$. The minimum stress of Design Set (1) is 41.2*MPa*, which is still very high for the epoxy based composite material, working around 80°C (refer to **Table 4**). No acceptable geometry design for the fuel cell plate can be achieved based on this selected materials. Modification on the material thus needs to be considered.

The material Design Set (2) applies both geometry parameters and material's Young's modulus *E* as design variables. The *E* is allowed to vary from 1 *GPa* to 10 *GPa*, while *W* and *H* can change over the same range as Design Set (1). For easily comparison, the optimization routine starts from the design optimum of the Design Set (1). The optimization routine converged at a minimum stress of 16.13 *MPa* with the geometry parameters $W = 0.00179\ m$, $H = 0.00199\ m$, and material parameter $E = 1.02\ GPa$, respectively. This result has acceptable stress/stain levels and geometry parameters.

Table 4: Design optimization of linear and nonlinear analysis

Design Set	Design Variables	Starting Point	Optimum	Minimal Stress
(1) Linear geometry design	W, H	($W = 0.001651\ m$, $H = 0.001778\ m$)	$W = 0.00153\ m$ $H = 0.00158\ m$	41.2 *MPa*
(2) Linear material design	W, H, E	($W = 0.00153\ m$, $H = 0.00158\ m$,E=3 *GPa*)	W=0.00179 *m* H=0.00199 *m* E=1.02 *GPa*	16.13 *MPa*
(3) Nonlinear geometry design	W, H	($W = 0.00153\ m$, $H = 0.00158\ m$)	W=0.000525 *m* H=0.00101 *m*	16.17 *MPa*

When applying design optimization through nonlinear FEA analysis, the material does not has to be changed, or the Young's modulus *E* of the material needs not to be modified, since the stress on the model simulation set (5) is only 17.74 *MPa*. Nonlinear geometry Design Set (3) uses the same geometry parameters and range of the Design Set (1) as design variables. The starting point of the search (*W* =0.00153 *m*, *H* = 0.00158 *m*) is the same optimum of Design Set (1) for the ease of comparison.

The optimization converged after iterations with the best design found at: wall thickness 0.525 *mm* and layer thickness 1.01 *mm*, which are at almost at the lower bounds of the two design variables and the design constraint, 1st principal strain 6615 $\mu\varepsilon$. The minimized objective function von Mises stress has been lowered to 16.17 *MPa*. All values at this design optimum are ideal for the fuel cell plate structure.

In summery, the optimal structure design of the fuel cell plates, which includes both geometry design and material design, provides abundant information on the plate geometry and corresponding material. Design Set (2) shows that the minimum stress level can be achieved with larger allowable geometry dimensions and lower Young's modulus material, given the linear material consideration. Design Set (3) indicates that acceptable stress values can also be obtained with smaller geometry dimensions under the assumption that the composite material possesses a nonlinear material property. The material does not have to be altered and an unchanged Young's modulus can be used.

The optimal structure design of the printed plate identifies the minimum maximum stress that can be used for the composite material, ensures that the maximum stress and strain are within the allowed range, and specifies the optimal plate geometry and material. These optimizations provide a broader scope to the feasible composite material, by identifying the lowest acceptable strength of the plate, in the channel material development. The optimizations also specify the corresponding stiffness relating to the Young's modulus of the composite material to be developed.

CONCLUSIONS

In this work, advanced computer modeling and finite element structure analysis are used as useful tools for the optimization of the plates at the early design stage. The design optimization provides a useful tool to combine both geometry and material designs for the plate structure to form a close form. Further study can be done to extend this new method, such as to use the volume of the flow channels of the plate as new design objective or constraint, to obtain a more practical design. The design analysis and optimization can provide guidelines for the development of the fuel cell plate and many other mechanical components of similar types.

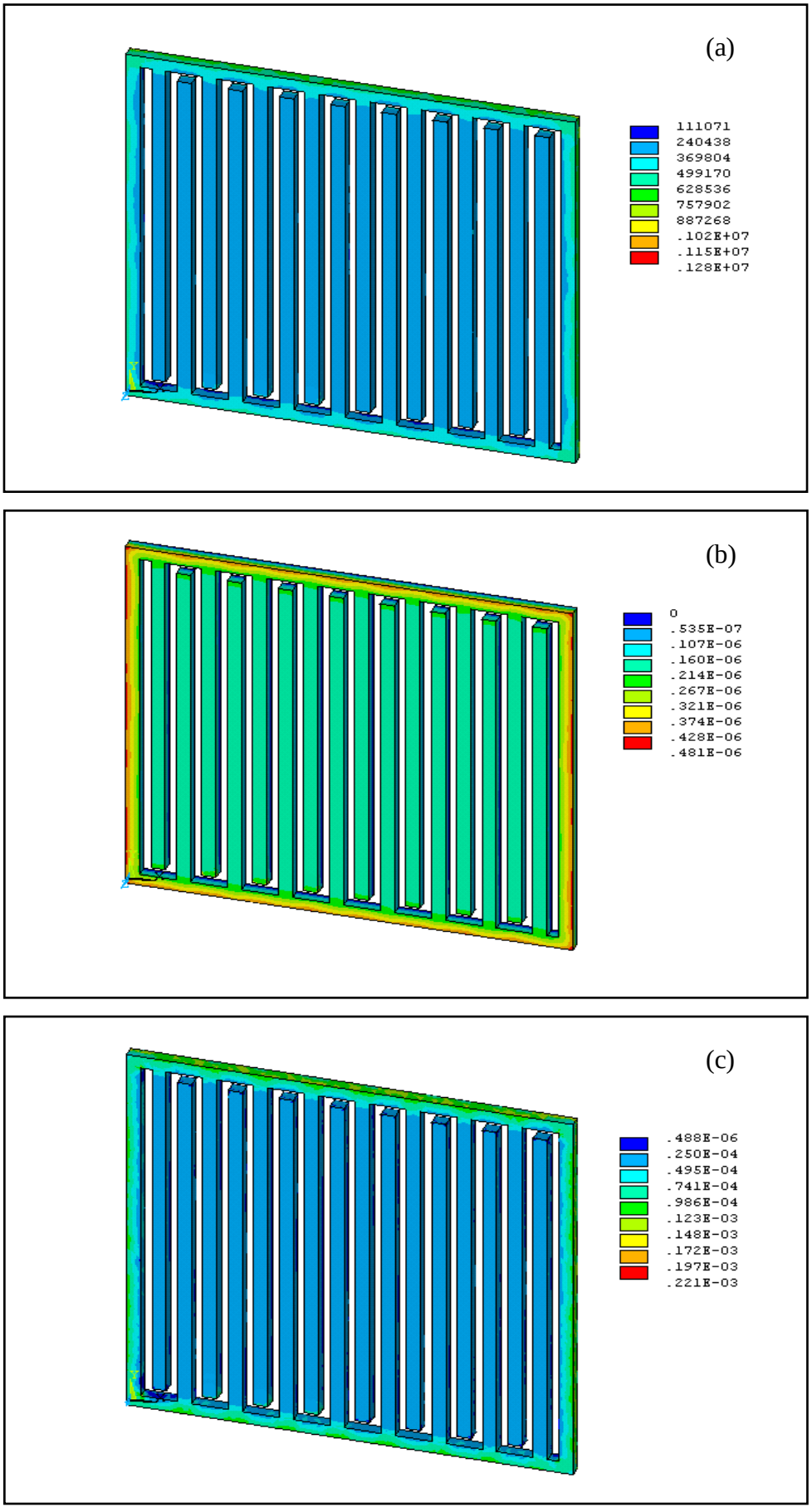

Fig. 6: Plate under pure structural loads. (a) Stress distribution. (b) Maximum displacement. (c) 1st principal strain.

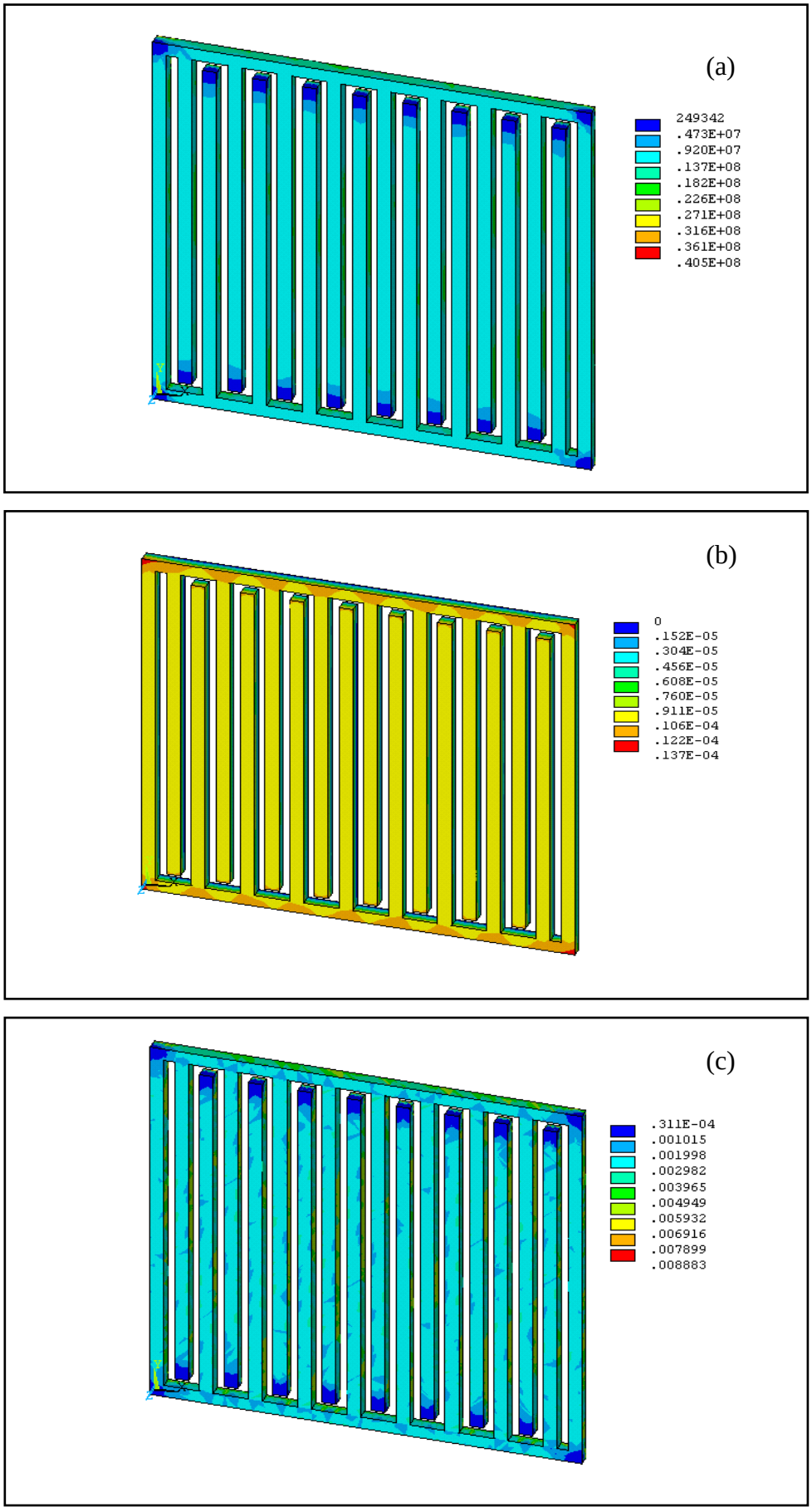

Fig. 7: Plate under temperature load only. (a) Stress distribution. (b) Maximum displacement. (c) 1st principal strain.

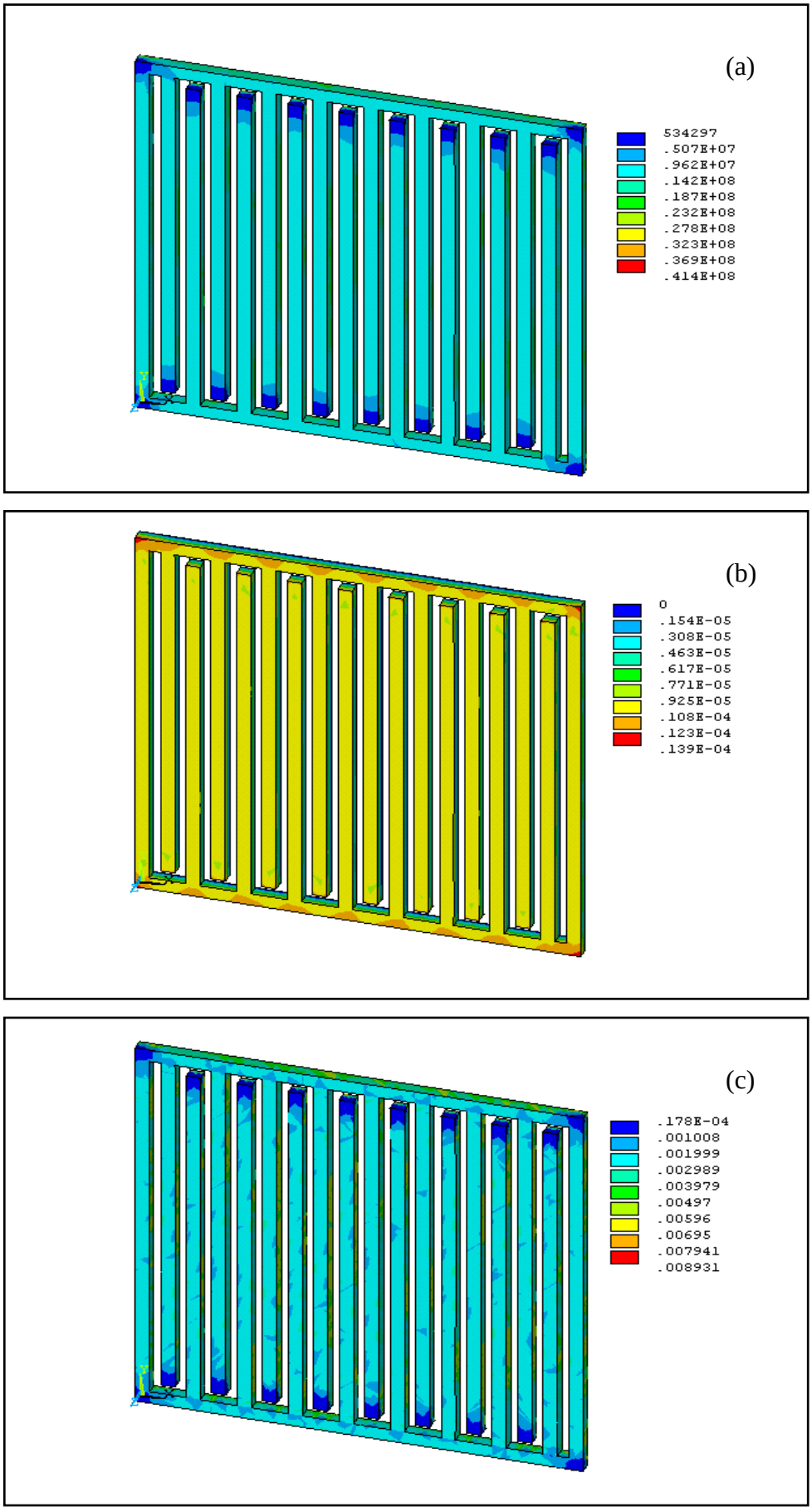

Fig. 8: Plate under structural and temperature loads. (a) Stress distribution. (b) Maximum displacement. (c) 1st principal strain.

References

Al-Hagag, Q. R., (2005) "Developing a model for thermodynamic analysis of a hydrogen-oxygen Fuel cell", MSc. Thesis , Babylon University, Iraq.

Busick, D.N. & Wilson, M.S., (1998) "Low-cost bipolar plates for PEFC stacks", Electrochemical Society Proceedings Volume 98-27. ISBN 1-56677-221-4.

Dong, Z.,(1999) "Fuel Cell Flow-Field Structure Formed by Layer Deposition," UK Patent GB 2336 712 A.

Davies, D.P., Adcock, P.L., Turpin, M. & Rowen, S.J., (2000). Stainless steel as bipolar plate material for solid polymer fuel cells. Journal of Power Sources, Vol. 86, No. 1-2, pp. 237-242. ISSN 0378-7753.

Larry, J. S.,(1984) "Applied Finite Element Analysis"

Menon, U., (1998) "Rapid Prototyping of Hardware and Software", Concurrent Design of Products, Manufacturing Processes and Systems, Gordon and Breach Science publishers.

Mennola, T. (2000) "Design and Experimental Characterization of Polymer Electrolyte Membrane Fuel Cells", MSc. Thesis, Helsinki University of Technology, Finland.

Onischak, M., Fan, Q., Chevrinko, J. & Marianovski, L.G.,(1999) " $10/kW bipolar plates for fuel cells" DOE/EPRI/GRI Fuel Cell Technology Review Conference. 3.-5.8. Chicago, Illinois, USA.

Pastula, M. E.,(1997)" Radiator Stack PEM Fuel Cell Architecture, System Modeling and Flow Field Design", M. A. Sc. Thesis, University of Victoria.

Perry, M. L., Newman, J., and Cairns, E. J.,(1998) "Mass Transport in Gas Diffusion Electrodes: A Diagnostic Tool for Fuel Cell Cathodes", Journal of the Electrochemical Society, v145, n1, p5-15.

Pirondi, A., Nicoletto, G., Cova, P., Pasqualetti, M., Portesine, M., and Zani, P. E.,(1998) "Thermo-Mechanical Simulation of a Multichip Press-Packed IGBT", Solid-State Electronics, v42, n12, p2303-2307.

Phong, T. Nguyen, Torston, B., Ned, D.,(2004) "Computential Model of a PEM Fuel Cell Serpentine Gas Flow Channels" Journal of Power Sources 130, p149-157.

Rao, S. S. , (1988) "The Finite Element Method in Engineering"

Reid C.E., Mérida W.R., McLean G., (1998) "Results and analysis of a PEMFC stack using metallic bi-polar plates'", In: Proceedings of the 1998 Fuel Cell Seminar, Palm Springs, California, USA. 16.-19.11.1998. United States Department of Defense.

Shi, L. T., and Tu, K. N.,(1995) "Finite Element Stress Analysis of Failure Mechanisms in a Multilevel Metallization Structure", Journal of Applied Physics, v77, n7.

NOTATIONS

D channel length
E Young's modulus
H thickness of printed layer
W channel wall thickness

X design variable

ε^1 maximum 1st principal strain

σ_{vm} maximum von Mises stress